Int. J. Heat Mass Transfer. Vol. 25, No. 4, pp. 523–534, 1982
Printed in Great Britain

0017–9310/82/040523–12 $03.00/0

RADIATIVE HEAT TRANSFER IN A COMPLETELY GENERAL PLANE-PARALLEL ENVIRONMENT

AJAY SHARMA and ALLEN C. COGLEY
Department of Energy Engineering, University of Illinois at Chicago Circle, P.O. Box 4348, Chicago, Illinois, U.S.A.

(*Received* 16 *January* 1981 *and in revised form* 23 *September* 1981)

Abstract—A new approach to radiative heat transfer with scattering is presented and used to obtain the first general solution for radiative equilibrium in a non-grey, plane-parallel medium. Use of the method when including conduction and convection is also discussed. Diffuse radiative fields are calculated in terms of defined scattering functions (Green's functions) that represent the response of the medium and any scattering (reflecting) surfaces to unitary-type illumination. These scattering functions are found using the computationally fast adding/doubling method. The energy conservation equation containing these scattering functions is then solved numerically for any particular heat transfer problem.

NOMENCLATURE

a, scattering functions defined in equations (22);
A_{ij}, elements of the integral equation kernels defined in equations (39);
$\mathbf{A}$, matrix of A_{ij};
$\mathbf{b}$, the Planck function vector defined in equation (39);
B, radiative source distribution;
$\bar{B}$, the Planck function;
c, scattering functions defined in equations (22);
E_1, the exponential integral function, degree 1;
f, the scattering kernel defined in equation (22);
$\mathbf{f}_{Ns}$, a vector of F_{Ns} defined in equations (39);
F_{Gs}, the function involving grey surface emissions defined in equation (32);
F_{Ns}, the function for non-grey surfaces given by equation (35);
g, asymmetry factor for the Henyey–Greenstein phase function, equation (33);
G, the kernel for the grey radiative equilibrium problem given in equation (31);
G_N, non-grey radiative equilibrium kernel defined in equation (37);
I, scalar specific intensity;
I_0^-, $I_{t_0}^+$, intensities originating at the top and bottom boundaries;
J, the scattering source function;
K_a, volumetric absorption coefficient;
$\bar{K}_a$, band averaged absorption coefficient, equation (42);
$\mathbf{K}_a$, the diagonal matrix of values of K_a at discrete space quadrature points;
K_p, the Planck mean absorption coefficient, equation (43);
K_s, volumetric scattering coefficient;
K_T, volumetric extinction coefficient;
P, the scattering phase function;
q_R, q_{RT}, the monochromatic, and total (summed for all wavelengths) radiative flux, respectively;
r, running optical depth variable, also the optical depth of the illumination;
R, temperature ratio T_B^4/T_T^4;
s, s', directions of radiative propagation, see Fig. 1;
t, t', optical depth variables;
t_0, total optical thickness of the medium;
$\mathbf{t}$, the vector of temperatures at discrete space quadrature locations;
T, $\bar{T}$, the transmission functions defined in equation (11) and Table 1, also T is used for the temperature where it is contextually clear;
T_B, T_T, the bottom and top surface temperatures, respectively;
$\mathbf{v}$, the "residual energy" vector given by equations (40) and (41);
w, standard space quadrature weights;
w_s, special (generalized) space quadrature weights;
x, y, z, space coordinates, see Fig. 1;
x_0, physical thickness of the medium.

Greek symbols

δ, the Dirac delta function;
ε_B, ε_T, emissivities of the bottom and top surfaces, respectively;
θ, zenith angle, see Fig. 1;
λ, the wavelength of radiation;
μ, cosine of the zenith angle;
ϕ, azimuth angle in Fig. 1, and the non-dimensional temperature defined in equation (30);
ω, single scattering albedo.

Subscripts

s, F,	standard and fundamental functions, respectively;
n,	nth Fourier component of a function.

Superscripts

+, −,	the direction of propagation of intensities and the direction of the *probe* (illumination) in the scattering and other functions;
0,	zeroth Fourier component;
n,	nth Fourier component.

INTRODUCTION

MANY RADIATIVE heat transfer problems in scattering, absorbing and emitting media have been solved under various simplifying assumptions. A good pedagogical summary of such solutions and their formulation is given by Sparrow and Cess [1]. Most of these solved problems are for grey, isotropically scattering, plane-parallel media with grey, diffuse surfaces [1–4]. However, approximate solutions are available for certain special cases such as media with specularly reflecting surfaces [5] and non-grey, but non-scattering, media with narrow spectral lines [6]. The usual approach adopted in obtaining these results involves simultaneous solution of the energy equation, radiative transfer equation, and radiative intensity balances at the reflecting surfaces. Without simplifying assumptions, the resulting coupled system of non-linear, integral–differential equations is extremely difficult to solve.

The solution procedure introduced here is conceptually quite different. Linearity of radiative transfer, with respect to radiative sources, is used to separate out all scattering phenomena by defining certain scattering functions that depend only upon medium and surface properties. This reduces the interdependence of the governing equations and allows one to handle all scattering events by means of an efficient matrix-algebra formulation. The scattering functions are generalizations of Chandrasekhar's [7] scattering and transmission functions and play the same role as Green's functions. A particular heat transfer problem is stated as a convolution (superposition) of the required radiative source distribution with the appropriate scattering functions. The resulting energy equation is then solved to obtain the needed temperature field and heat fluxes. The structure of this formulation leads naturally to general and automated numerical solutions. Although here restricted to plane-parallel media, the same concept should be extendible to multi-dimensional problems.

As a particular application this paper presents the first general solution for non-grey radiative equilibrium with scattering. The solution applies to anisotropically scattering, inhomogeneous media with arbitrary reflecting and absorbing surfaces. The solution procedure is general enough in that it also can be used for problems with conduction and convection.

DIFFUSE RADIATIVE FIELDS

The background for the scattering radiative transfer used in this paper is developed in [8–12]. The important attributes of this approach are (1) it collects all scattering phenomena into a set of scattering functions that depend only upon medium and surface properties, and (2) these functions are calculated by a fast adding/doubling algorithm which is purely algebraic. The radiative heat flux can then be expressed by convoluting the radiative sources with the scattering functions. This process replaces the usual procedure of solving a coupled set of integral equations representing radiative transfer. With the present formulation, only the single energy equation must be solved for any given heat transfer problem. A brief description of the method follows, while the details are available in [8].

Consider phase incoherent, monochromatic radiation represented by the scalar specific intensity* I in a plane-parallel, finite medium. The origin of the Cartesian coordinate is at the top boundary with x measured positively into the medium as shown in Fig. 1. Direction of radiative propagation at a point is given by $s(\theta, \phi)$, the set of zenith θ and azimuthal ϕ angles referenced to the x and y directions, respectively. The volumetric absorption K_a and scattering K_s coefficients and their sum (extinction coefficient) $K_T = K_a + K_s$ can vary only with x†. The dimensionless optical depth is defined on the extinction coefficient as

$$t = \int_0^x K_T(x')\,dx', \tag{1}$$

and t_0 and x_0 are the total optical depth and thickness, respectively. With this nomenclature, the equation of radiative transfer can be written as [1]

$$\mu \frac{\partial I(t, s)}{\partial t} = I(t, s) - B(t, s) - J(t, s) \tag{2}$$

where $\mu = \cos\theta$ is the zenith direction cosine. The internal radiative source distribution B is defined such that

$$B(t, s)\left|\frac{dt}{\mu}\right|$$

yields the specific intensity in direction s illuminating the medium at t due to sources in dt. For thermal sources at local thermodynamic equilibrium one obtains

$$B(t) = [1 - \omega(t)]\,\bar{B}[T(t)], \tag{3}$$

where $\bar{B}$ is the Planck function at temperature T and ω

* The notation here does not explicitly note the frequency dependence of I and other variables and parameters. It is understood that the monochromatic problem is being developed at this point.

† Radiative properties are usually known functions of the temperature. For heat transfer problems with sufficient temperature variations, the medium properties become functions of the unknown temperature field. We deal only with temperature independent radiative properties here and point out in the next section how this constraint can be relaxed.

$= K_s/K_T$ is the albedo for single scattering. The scattering source function J is then defined by

$$J(t, s) = \frac{\omega(t)}{4\pi} \int_{-1}^{1} d\mu' \int_{0}^{2\pi} d\phi' \, P(t; s, s') \, I(t, s'), \quad (4)$$

where P is the scattering phase function normalized such that

$$\int_{-1}^{1} d\mu' \int_{0}^{2\pi} d\phi' \, P(t; s, s') = 4\pi. \quad (5)$$

For convenience the radiative field is split into the positive (up) and negative (down) hemispherical directions and consequently all μ's are read as positive. Equation (2) is solved by an integrating factor to obtain the following expressions for the upward I^+ and downward I^- propagating intensities:

$$I^+(t, s) = I^+_{t_0}(s) \exp\left(\frac{t - t_0}{\mu}\right) + \frac{1}{\mu} \int_{t}^{t_0} dt' \, [B(t', s) + J(t', s)] \exp\left(\frac{t - t'}{\mu}\right) \quad (6)$$

and

$$I^-(t, s) = I^-_0(s) \exp\left(-\frac{t}{\mu}\right) + \frac{1}{\mu} \int_{0}^{t} dt' \, [B(t', s) + J(t', s)] \exp\left(\frac{t' - t}{\mu}\right). \quad (7)$$

Here I^-_0 and $I^+_{t_0}$ are intensities emitted at the top and bottom surfaces, respectively.

The traditional approach is to now combine equations (4), (6) and (7) to derive an integral equation for J, and this equation is solved simultaneously with the energy equation (see, e.g., Ch. 7 of [1]). In the present work a different approach is taken. The integral equation for J, along with distribution theory, is used to obtain the following statement of linearity [12]:

$$J(t, s) = \frac{1}{4\pi} \int_{0}^{1} d\mu' \int_{0}^{2\pi} d\phi' \left\{ I^+_{t_0}(s') \, J^+_s(t, s; t_0, s') + I^-_0(s') \, J^-_s(t, s; t_0, s') + \frac{1}{\mu'} \int_{0}^{t_0} dt' \left[B^+(t', s') \, J^+_F(t, s; t_0, s', t') + B^-(t', s') \, J^-_F(t, s; t_0, s', t') \right] \right\}. \quad (8)$$

This equation expresses the fact that the scattering source function can be expressed as convolutions of the driving illumination with the functions J_F and J_s. These functions are Green's functions that characterize the response of the scattering environment to unitary-type probes. The fundamental or Green's problem is specified by the following illumination:

$$I^+_{t_0} = I^-_0 = 0,$$
$$B(t, s) = 4\pi\mu \, \delta(s - s', t - t') \quad (9)$$

where δ is the Dirac delta function. The solution to this problem is J_F and, when the probe is at a boundary, J_s.

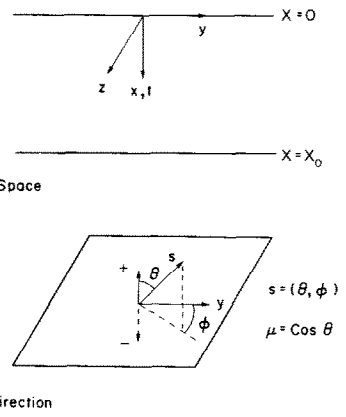

FIG. 1. The coordinate nomenclature.

An important concept of nomenclature should be made clear. The superscript sign on a resulting or driving intensity is the direction of propagation. The resulting or required scattering source function J is also an intensity and fits the same scheme. However, the J_F's and J_s's are intermediate Green's function that depend upon two directions, one for radiative propagation (response) and the other for the illumination (probe). The superscript signs on these functions, and the related scattering functions that follow, denote the direction of *illumination*.

The source function is a local point function of which only certain spatial integrals are required to obtain the radiative intensities. This is observed by substituting equation (8) into equation (6) to obtain

$$I^+(t, s) = I^+_{t_0}(s) \exp\left(\frac{t - t_0}{\mu}\right) + \frac{1}{4\pi\mu} \int_{t}^{t_0} dt' \exp\left(\frac{t - t'}{\mu}\right) \int_{0}^{1} d\mu' \int_{0}^{2\pi} d\phi' \times \left\{ I^+_{t_0}(s') \, J^+_s(t', s; t_0, s') + I^-_0(s') \, J^-_s(t', s; t_0, s') + \frac{1}{\mu'} \int_{0}^{t_0} dr \, [B^+(r, s') \, J^+_F(t', s; t_0, s', r) + B^-(r, s') \, J^-_F(t', s; t_0, s', r)] \right\}. \quad (10)$$

This expression contains the following scattering functions

$$\bar{T}^+_F(t, s; t_0, s', r) = \int_{t}^{t_0} dt' \exp\left(\frac{t - t'}{\mu}\right) J^+_F(t', s; t_0, s', r),$$
$$\bar{T}^-_F(t, s; t_0, s', r) = \int_{0}^{t} dt' \exp\left(\frac{t' - t}{\mu}\right) J^-_F(t', s; t_0, s', r),$$
$$\bar{S}^+_F(t, s; t_0, s', r) = \int_{0}^{t} dt' \exp\left(\frac{t' - t}{\mu}\right) J^+_F(t', s; t_0, s', r),$$
$$\bar{S}^-_F(t, s; t_0, s', r) = \int_{t}^{t_0} dt' \exp\left(\frac{t - t'}{\mu}\right) J^-_F(t', s; t_0, s', r) \quad (11)$$

and their spatial limits [10–12] given in Table 1. These functions are global in that they represent scattering processes in a finite layer of optical thickness t_0,

Table 1. Role of scattering functions

Level	Function group	Role: Observer	Role: Probe
3	$\bar{S}_F^{\pm}, \bar{T}_F^{\pm}(t, s; t_0, s', r)$	interior (t, s)	interior (s', r)
2	$\bar{S}_s^{\pm}, \bar{T}_s^{\pm}(t, s; t_0, s')$	interior (t, s)	boundary $\begin{pmatrix} s', & r \to 0 \\ & r \to t_0 \end{pmatrix}$
2	$S_F^{\pm}, T_F^{\pm}(s; t_0, s', r)$	boundary $\begin{pmatrix} t \to 0 \\ t \to t_0 \end{pmatrix}, s$	interior (s', r)
1	$S_s^{\pm}, T_s^{\pm}(s; t_0, s')$	boundary $\begin{pmatrix} t \to 0 \\ t \to t_0 \end{pmatrix}, s$	boundary $\begin{pmatrix} s', & r \to t_0 \\ & r \to 0 \end{pmatrix}$

together with any effects of boundary reflections as explained in [10]. In equations (11), T stands for transmission functions where radiation is diffusely transmitted in the direction of probe, while S is a scattering function which represents the same scattering phenomena for the direction opposite to the probe. All such functions are generally called "scattering" functions. Using these functions, the intensity fields of equations (6) and (7) can be written as

$$I^+(t) = I^+_{t_0} \exp\left(\frac{t - t_0}{\mu}\right) + \frac{1}{4\pi\mu}\left\{\int_0^1 d\mu' \int_0^{2\pi} d\phi' \left[I^+_{t_0} \bar{T}^+_s(t) + I^-_0 \bar{S}^-_s(t) + \frac{1}{\mu'}\int_0^{t_0} dr\,(B^+(r)\,\bar{T}_F(t, r) + B^-(r)\,\bar{S}^-_F(t, r))\right]\right\} \tag{12}$$

$$I^-(t) = I^-_0 \exp\left(-\frac{t}{\mu}\right) + \frac{1}{4\pi\mu}\left\{\int_0^1 d\mu' \int_0^{2\pi} d\phi' \left[I^+_{t_0} \bar{S}^+_s(t) + I^-_0 \bar{T}^-_s(t) + \frac{1}{\mu'}\int_0^{t_0} dr(B^+(r)\,\bar{S}^+_F(t, r) + B^-(r)\,\bar{T}^-_F(t, r))\right]\right\}. \tag{13}$$

In these equations, and in many instances to follow, the directional (angular) dependence of various functions has been omitted for brevity.

A Fourier series expansion for the ϕ dependence of all intensities and scattering functions is next introduced to simplify calculations. It will also be shown that heat transfer problems involve only the zeroth Fourier components. The scattering phase function P is expanded as

$$P(t; s, s') = \sum_{n=0}^{N} P_n(t; \mu, \mu') \cos n(\phi - \phi'). \tag{14}$$

Intensities and sources are similarly represented by

$$I(t, s) = \sum_{n=0}^{N} I^n(t, \mu) \cos n\phi, \qquad B(t, s) = \sum_{n=0}^{N} B_n(t, \mu) \cos n\phi. \tag{15}$$

Fourier components of the scattering functions are also defined, e.g.:

$$T^+_s(s; t_0, s') = \sum_{n=0}^{N} T^{n+}_s(\mu; t_0, \mu') \cos n(\phi - \phi'). \tag{16}$$

Algebraic substitution of these expressions into the preceding development shows that each Fourier component of the intensity field depends only upon corresponding components of the scattering functions.

Heat transfer problems require the radiant heat flux and its divergence, which in one dimension is the partial derivative of heat flux with respect to the optical depth. Heat flux divergence is used in the energy conservation equation which is solved to obtain the temperature distribution. In most engineering problems, once the temperature profile is known, the heat flux is required only at medium boundaries. The flux at the boundaries can be written in terms of lower level scattering functions than the internal flux in the medium. To determine which scattering functions are needed for heat transfer calculations, heat flux expressions are developed.

The monochromatic radiative flux q_R is given by the angular integration of intensity as

$$q_R(t) = \int_{4\pi} ds\,\mu I(t, s) = \int_{-1}^{1} \mu d\mu \int_0^{2\pi} d\phi \left[\sum_{n=0}^{N} I^n(t, \mu) \cos n\phi\right] = 2\pi \int_{-1}^{1} \mu d\mu\, I^0(t, \mu). \tag{17}$$

Therefore, one obtains

$$q_R(t) = 2\pi \int_0^1 \mu d\mu\,[I^{0-}(t, \mu) - I^{0+}(t, \mu)]. \tag{18}$$

Suitable expressions of intensities [e.g. the zeroth Fourier components from equations (12) and (13)] can be substituted in (17) to calculate the heat flux. This has been done in Ch. IV of [8]. In order to formulate the heat transfer problem, equation (17) is differentiated to obtain the expression for the divergence of q_R as

$$\frac{\partial q_R(t)}{\partial t} = \int_{4\pi} ds\,\mu \frac{\partial I(t, s)}{\partial t}. \tag{19}$$

The governing equation (2) of radiative transfer is then used to obtain

$$\frac{\partial q_R(t)}{\partial t} = \int_{4\pi} ds\,[I(t, s) - B(t, s) - J(t, s)]. \quad (20)$$

The scattering source function J can be eliminated from (20) in terms of the intensity field I. First, the following expression of energy conservation is derived by integrating the defining equation (4) for J and using the normalization (5) of the scattering phase function:

$$\int_{4\pi} ds\, J(t, s) = \frac{\omega(t)}{4\pi} \int_{4\pi} ds \int_{4\pi} ds'\, P(t; s, s')\, I(t, s')$$

$$= \frac{\omega(t)}{4\pi} \int_{4\pi} ds' \left[\int_{4\pi} ds\, P(t; s, s') \right] I(t, s')$$

$$= \omega(t) \int_{4\pi} ds'\, I(t, s').$$

This relation used in equation (20) then gives

$$\frac{\partial q_R(t)}{\partial t} = \int_{4\pi} ds \{[1 - \omega(t)]\, I(t, s) - B(t, s)\}. \quad (21)$$

It is seen therefore, that both the heat flux q_R and its divergence are expressible in terms of angle integrals of I. This leads to the definition of the following angle-integrated scattering functions:

$$c^+(t, \mu; t_0) = \frac{2\pi}{\mu} \int_0^1 \frac{d\mu'}{\mu'} [\bar{T}_s^{0-}(t, \mu; t_0, \mu') + \bar{S}_s^{0-}(t, \mu; t_0, \mu')],$$

$$c^-(t, \mu; t_0) = \frac{2\pi}{\mu} \int_0^1 \frac{d\mu'}{\mu'} \times [\bar{T}_s^{0+}(t, \mu; t_0, \mu') + \bar{S}_s^{0+}(t, \mu; t_0, \mu')],$$

$$a^+(t, \mu; t_0, r) = 2\pi \int_0^1 \frac{d\mu'}{\mu'} \times [\bar{T}_F^{0+}(t, \mu; t_0, \mu', r) + \bar{S}_F^{0-}(t, \mu; t_0, \mu', r)],$$

$$a^-(t, \mu; t_0, r) = 2\pi \int_0^1 \frac{d\mu'}{\mu'} \times [\bar{T}_F^{0-}(t, \mu; t_0, \mu', r) + \bar{S}_F^{0+}(t, \mu; t_0, \mu', r)]$$

and

$$f^{\pm}(t; t_0, r) = \frac{1}{4\pi} \int_0^1 \frac{d\mu}{\mu} \times [a^-(t, \mu; t_0, r) \pm a^+(t, \mu; t_0, r)]. \quad (22)$$

These definitions are used, together with the intensity field expressions (12) and (13) in equation (21) to obtain the expression for the monochromatic radiative heat flux divergence for thermally illuminated media [8] as

$$\frac{\partial q_R(t)}{\partial t} = 2\pi[1 - \omega(t)] \left\{ -2\bar{B}(t) + \int_0^{t_0} dt' [1 - \omega(t')]\, \bar{B}(t') [E_1(|t - t'|) + f^+(t, t')] + \int_0^1 d\mu\, I_{t_0}^{0+} \left[\exp\left(\frac{t - t_0}{\mu}\right) + \frac{c^-(t, \mu)}{4\pi} \right] + \int_0^1 d\mu\, I_0^{0-} \left[\exp\left(\frac{-t}{\mu}\right) + \frac{c^+(t, \mu)}{4\pi} \right] \right\}. \quad (23)$$

Boundary intensities I_0^{0-} and $I_{t_0}^{0+}$ appearing in (23) are considered to be functions of μ, allowing for anisotropic boundary conditions. No assumption has been made about scattering within the medium, which can also be anisotropic. The function E_1 appearing above is the standard exponential integral function.

It is clear from equation (23) that in the present formulation, the temperature field (contained in $\bar{B}$) has been separated from the scattering phenomena. *All* scattering processes are represented by the scattering functions which are calculated in terms of the media scattering properties only, and are therefore independent of the illumination.

CALCULATING THE SCATTERING FUNCTIONS

The scattering functions S, T, c, a and f defined in the previous section depend upon the single scattering albedo ω and the phase function P. They are independent of the radiative source function B if ω and P are. In the case of thermally driven media, the scattering functions can be independently calculated if ω and P are not temperature dependent. However, if the radiative properties vary with temperature, the procedure for obtaining the scattering functions described below has to be applied iteratively with the solution of the energy equation [8].

Domanus and Cogley [12] developed an invariant imbedding method for computing the scattering functions. Their work used parametric differentiation with respect to optical thickness to replace the governing linear integral equation for the scattering function by a set of ordinary differential equations appropriate for numerical integration. Invariant imbedding equations result in exact calculation of the scattering functions for inhomogeneous media [13]. This method, however, requires the solution of a very large system of simultaneous, non-linear, ordinary differential equations, making the computations rather slow [8]. Therefore, the adding method was adopted [8–10] as an alternative, fast scheme of obtaining the scattering functions.

The adding/doubling method has been developed by several investigators [14, 15] using seemingly different approaches and nomenclature. It has been widely used because it is computationally fast and accurate for homogeneous scattering media. To apply the adding method to inhomogeneous media, small homogeneous layers with different scattering properties are superimposed, resulting in some errors in the scattering functions. These errors have only recently been characterized, and criteria for controlling them have been developed [16]. This has been done by having an adding/doubling scheme which parallels the exact invariant imbedding method of [12]. Thus, it has been

shown [16] that the adding/doubling algorithm can calculate the scattering functions necessary for heat transfer problems, to within an accuracy of 1%, in less than $\frac{1}{5}$ the computer time required by the corresponding invariant imbedding calculations.

The adding method used in the present work is derived from the superposition principle using the statement of linearity in scattering phenomena given in equation (8). It is beyond the scope of this paper to describe adding/doubling in detail. All the adding equations for the scattering functions and the details of the algorithm used are available in [8] and [10]. The important points to note about this technique are: (1) it allows for calculations of all the scattering functions introduced in the previous section in terms of the media radiative properties ω, P and the optical thickness; (2) these calculations are exact for homogeneous media and accurate, with controlled error, for inhomogeneous media, and (3) all scattering phenomena, including surface scattering, are represented by the calculated scattering functions. Unlike many other techniques, the present approach decouples scattering (reflection) processes occurring on the boundary surfaces from the surface radiocities. The adding/doubling scheme incorporates the effects of completely general surfaces on the scattering functions in a straightforward and unified manner [8–10].

A fast production level adding/doubling computer program for scattering function calculations is available from the authors. Therefore, these calculations can be thought of as being performed by a "black box" with radiative properties as input and scattering functions as output.

RADIATIVE EQUILIBRIUM

When radiation is the only, or predominant, mode of energy transfer and the system is in steady state, the energy equation reduces to

$$\operatorname{div} q_{RT} = 0. \tag{24}$$

This defines the condition of radiative equilibrium. For the 1-dim. geometry (Fig. 2) considered in this paper, radiative equilibrium is represented by

$$\frac{dq_{RT}}{dx} = 0. \tag{25}$$

Here q_{RT} is the total radiative heat flux that is related to the monochromatic quantity discussed earlier by

$$q_{RT} = \int_0^\infty q_R(\lambda)\, d\lambda, \tag{26}$$

where λ is the wavelength of radiation. Therefore the condition for radiative equilibrium can be written as

$$\int_0^\infty \frac{\partial q_R(\lambda)}{\partial x}\, d\lambda = 0. \tag{27}$$

Using the chain rule of differentiation and definition (1) for optical depth t, (27) can be rewritten as

$$\int_0^\infty K_T(\lambda, x)\frac{\partial q_R}{\partial t}(\lambda, x)\, d\lambda = 0, \tag{28}$$

where K_T is the extinction coefficient defined earlier. The expression (23) for $\partial q_R/\partial t$ is then substituted into (28). Before dealing with this rather complex non-grey problem, the simple case of a grey medium is considered.

A medium is grey when its radiative properties are not functions of the wavelength. If the surfaces are also assumed to be grey with directional emissivities ε_T and ε_B at temperatures T_T and T_B, respectively, the radiative equilibrium equation can be written as

$$2\phi(t) = F_{Gs}(t) + \int_0^{t_0} G(t, t')\,\phi(t')\, dt. \tag{29}$$

The Planck function has been frequently integrated as

$$\int_0^\infty \bar{B}(\lambda, T)\, d\lambda = \frac{\sigma T^4}{\pi},$$

where σ is the Stefan–Boltzmann constant. In equation (29) the non-dimensional temperature function ϕ is defined by

$$\phi(t) = \frac{T^4(t) - T_T^4}{T_B^4 - T_T^4}, \tag{30}$$

and the kernel G can be written as

$$G(t, t') = [1 - \omega(t')]\,[E_1(|t - t'|) + f^+(t, t')]. \tag{31}$$

Finally, the inhomogeneous function F_{Gs} is found to be

$$F_{Gs}(t) = \frac{1}{1-R}\left\{\int_0^1 \varepsilon_B(\mu)\left[\exp\left(\frac{t-t_0}{\mu}\right) + \frac{c^-(t,\mu)}{4\pi}\right]d\mu + R\left(\int_0^1 \varepsilon_T(\mu)\left[\exp\left(-\frac{t}{\mu}\right) + \frac{c^+(t,\mu)}{4\pi}\right]d\mu + \int_0^{t_0} G(t, t')\, dt' - 2\right)\right\}, \tag{32}$$

where $R = T_B^4/T_T^4$.

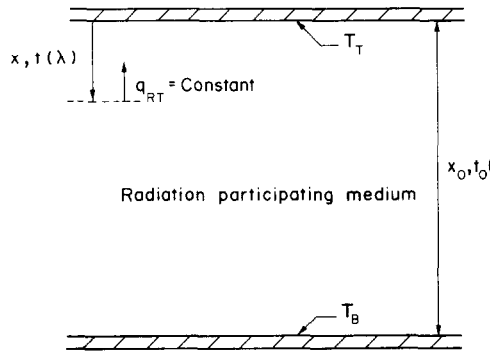

FIG. 2. A schematic for plane-parallel radiative equilibrium.

Equation (29) is similar to the corresponding equation for isotropic scattering given as equation (8–4) of [1], and reduces to that equation when scattering is isotropic and surfaces are diffuse. Although the analytic reduction of equation (29) to equation (8–4) of [1] is rather involved and tedious, the numerical solutions discussed later demonstrate this reduction. Anisotropic scattering introduces the c scattering functions in F_{Gs} and the f^+ function in the kernel G. Also note that anisotropic scattering does not allow one to define ϕ in terms of surface radiosities as in [1]. Consequently the solution of ϕ depends upon the temperature ratio R. Nonetheless, all grey radiative equilibrium problems in plane-parallel media are governed by an integral equation of the same form.

The equation (29) for radiative equilibrium is a Fredholm integral equation of the second kind. Although several solution techniques exist for integral equations, a numerical scheme is used here for two reasons. First of all, no exact analytic solution of the above equations is possible, while accurate numerical results are obtained economically. Secondly, since the c and f^+ scattering functions can only be calculated numerically and at discrete optical depth locations, numerical solutions of integral equations containing them are imperative. The integral equation is converted to a discrete form since the unknown function ϕ can only be calculated at a finite number of locations. This is done by replacing the integral appearing in (29) by a numerical quadrature. A special quadrature scheme is used to accurately handle the singular E_1 function present in the integrand. In this scheme the quadrature weights are functions of moments of the E_1 function, and the singular part of the integrand is thus analytically integrated. Once converted to a discrete form, the governing integral equation (29) reduces to a set of simultaneous, linear, algebraic equations which are then solved in a standard manner. The details of the special quadrature and the numerical method are available in [17], which also contains a discussion on the accuracy of this approach. Example results for grey radiative equilibrium with anisotropic scattering and reflecting boundaries are presented here. In these examples, the scattering phase function used is the one developed by Henyey and Greenstein [18]. This analytic phase function simulates aerosol scattering quite well while being simple and computationally efficient to use. The phase function is given by

$$P(\Theta, g) = \frac{1 - g^2}{(1 + g^2 - 2g \cos \Theta)^{3/2}}. \qquad (33)$$

Here Θ is the included angle between the incident and scattered rays, and the parameter g is the asymmetry factor. The value $g = 0$ represents an isotropic scatterer, $0 < g \leq 1$ a forward scatterer, and $-1 \leq g < 0$ gives backward scattering. The extreme values of g, 1 and -1, are used for total forward or backward scattering, respectively.

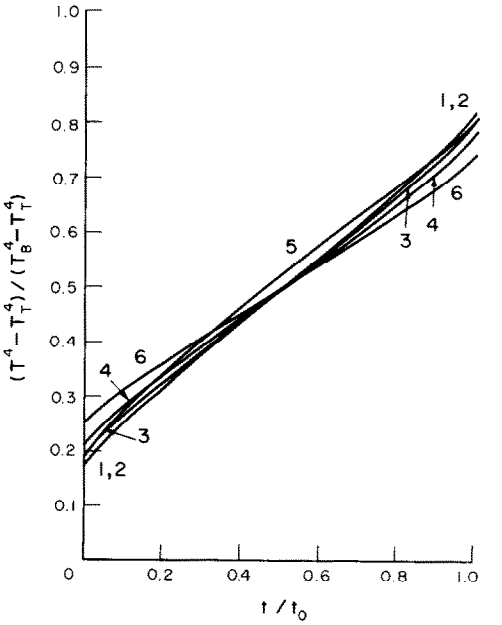

FIG. 3. Temperature as a function of optical depth t for grey radiative equilibrium with $R = 0.01$ and $t_0 = 2.0$. The curves correspond to: (1) $\omega = 0.4, g = 0.0$; (2) $\omega = 0.4t, g = 0.0$; (3) $\omega = 0.4, g = 0.4$; (4) $\omega = 0.4, g = 0.8$; (5) $\omega = 0.4, g = 0.4t$. Curves 1–5 are for black surfaces while curve 6 has medium properties as in curve 1 with reflecting surface properties given in Fig. 4.

The results in Fig. 3 show the effects of anisotropic scattering and reflecting surfaces on radiative equilibrium temperature profiles in grey media of $t_0 = 2.0$ with grey surfaces and $R = 0.01$. Curves 1–5 are for media with black surfaces while curve 6 is for a homogeneous, isotropic ($\omega = 0.4$, $g = 0.0$) medium bounded by identical reflecting surfaces at the top and bottom with the properties given in Fig. 4. In Fig. 3, curve 1 is for a homogeneous and isotropic medium of $\omega = 0.4$ and $g = 0$. This curve reproduces the results for isotropic scattering media given in [1] and, therefore, confirms the accuracy of present calculations. Curve 2 is calculated for a medium of isotropic scatterers which are inhomogeneously distributed ($\omega = 0.4t$). The theory of isotropic

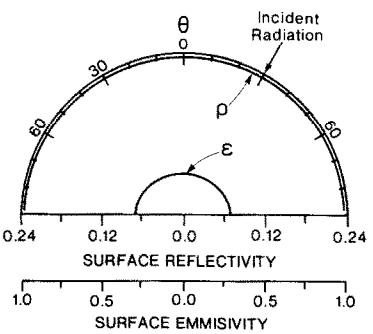

FIG. 4. The bidirectional reflectivity ρ for the incidence angle shown, and the corresponding emissivity ε, for the opaque surfaces used in Fig. 3, curve 6.

scattering [1] contends that the conditions of radiative equilibrium are independent of ω for such media. In Fig. 3, curves 1 and 2 are identical, thus confirming that proper numerical cancellation of the terms involving ω is taking place. In fact the numerical results used to plot curves 1 and 2 are the same to three significant digits. The temperature profiles for anisotropic scattering media of $\omega = 0.4$ are shown in curves 3 ($g = 0.4$), 4($g = 0.8$) and 5 ($g = 0.4t$). The scatterers used for curve 5 have different phase function at different locations as given by the g profile. These three curves (3, 4 and 5) show that the anisotropy of the scattering phase function can significantly perturb the radiative equilibrium temperature profile. Forward scatterers ($g > 0$) are seen to increase the temperature difference (radiation slip) between the boundary surfaces and the medium next to them (compare the end points of curves 1, 3 and 4). Surface scattering (reflection) is seen to have the same effect (curve 6), and these changes are similar to those which occur if the medium optical thickness t_0 is reduced. All media with symmetry about the centerline have the same centerline temperature ($\phi_{\text{center}} = 0.5$). Although this symmetry is not disturbed by variations in ω for isotropic scatterers, the situation with inhomogeneously distributed anisotropic scatters ($g = 0.4t$) is not symmetric (curve 5), and $\phi_{\text{center}} \neq 0.5$.

For the special case of one black surface and one specularly reflecting surface with an isotropically scattering medium, a prior solution for grey radiative equilibrium exist and is discussed in [1]. In that case (his Figs. 8-7 and 8-8) the temperature profiles are normalized with radiosities and show a much smaller surface reflecting effect and in the opposite sense when compared to curve 6 of Fig. 3. The actual temperature profiles are presented here and show the fact that reflecting surfaces increase the radiation slip. This phenomena is correct since in the limit of completely reflecting surfaces (a limit that must be taken with care and is in a sense nonphysical) the solution is ϕ = constant = 0.5.

The next step is to consider the realistic situation of radiative equilibrium in absorbing, emitting, and anisotropically scattering media with wavelength dependent properties. Equation (23) is used together with the expression (28) resulting in the following governing equation for non-grey radiative equilibrium:

$$\int_0 K_a(\lambda, x)\left\{-2\bar{B}[\lambda, T(x)] + F_{Ns}(\lambda, x) + \int_0^{x_0} G_N(\lambda, x, x')\bar{B}[\lambda, T(x')]\,dx'\right\}d\lambda = 0. \quad (34)$$

Here x is the physical space coordinate as illustrated in Fig. 2, and K_a is the volumetric absorption coefficient for the medium which appears here because

$$K_T(1-\omega) = (K_a + K_s)\left(1 - \frac{K_s}{K_a + K_s}\right) = K_a.$$

The temperature T is the dependent variable and $\bar{B}$ is the Planck function at wavelength λ. The driving function F_{Ns} is given by

$$F_{Ns}(\lambda, x) = \int_0^1 d\mu \left\{ I_{t_0}^{0+}\left[\exp\left(\frac{t - t_0}{\mu}\right) + \frac{c^-(t, \mu)}{4\pi}\right] + I_0^{0-}\left[\exp\left(-\frac{t}{\mu}\right) + \frac{c^+(t, \mu)}{4\pi}\right]\right\}. \quad (35)$$

The optical depth coordinate t appearing on the R.H.S. of (35) is mapped to the physical depth x by equation (1). For the special case of media bounded by surfaces at temperatures T_T and T_B, the first Fourier component of the boundary intensities are calculated from

$$\begin{aligned} I_{t_0}^{0+}(\lambda, \mu) &= \varepsilon_B(\lambda, \mu)\bar{B}(\lambda, T_B), \\ I_0^{0-}(\lambda, \mu) &= \varepsilon_T(\lambda, \mu)\bar{B}(\lambda, T_T). \end{aligned} \quad (36)$$

Here ε are the directional spectral emissivities of the surfaces. The kernel G_N in Equation (34) is written in terms of previously defined functions as

$$G_N(\lambda, x, x') = K_a(\lambda, x')[E_1(|t - t'|) + f^+(t, t')]. \quad (37)$$

The above expression also employs the mapping from x to t coordinates. To clarify this transformation, equation (1) is restated here in the following form:

$$t(\lambda, x) = \int_0^x K_T(\lambda, x')\,dx'. \quad (38)$$

Thus, for example, to calculate $G_N(\lambda, x, x')$, first the optical depths t and t' corresponding to x and x', respectively, are obtained from (38). Then the E_1 and f^+ functions for these optical depths are used in equation (37). A similar procedure is used with equation (35).

Equation (34) is the expression of conservation of total radiant energy in non-grey media. The terms within the braces calculate the efflux of energy from a fluid element, and the influx from the rest of the medium and boundaries, at a particular wavelength. The outer frequency integration denotes that in a non-grey medium the first law of thermodynamics requires only that the sum over all wavelengths of these interchanges be zero. Therefore, equation (34) is an integral over λ of non-linear Fredholm integral equations in T. No direct analytic or numerical solution of this equation is possible. However, an iterative solution method can be used, and an efficient scheme for that is detailed in [17]. In summary the governing equation (34) is first modified for discrete space coordinates in a manner similar to that described previously for the grey medium equation.

The quadrature scheme used for the space integration is the same as that used before, and the following vectors and matrices are defined:

$\mathbf{K_a}(\lambda)$: a diagonal matrix of absorption coefficients $K_a(\lambda, x_i)$,

$\mathbf{b}(\lambda)$: the Planck function vector of the unknown

temperature $T_i = T(x_i)$, such that its components are given by $b_i(\lambda) = \bar{B}(\lambda, T_i)$,

$\mathbf{f}_{Ns}(\lambda)$: a vector with components given by $f_{Ns_i} = F_{Ns}(\lambda, x_i)$,

and the matrix

$$\mathbf{A}(\lambda) = [A_{ik}(\lambda)],$$

where

$$A_{ik}(\lambda) = K_a(\lambda, x_k)[w_{s_{ik}}(\lambda) + w_{ik} f^{+}_{ik}(\lambda)]. \quad (39)$$

The quadrature weights w_{ik} are the standard (e.g. Simpson's rule) weights, and $w_{s_{ik}}$ are the special weights [17] used for the singular part of the integrand. Equation (34) is now rewritten as:

$$\int_0^{x} \mathbf{K}_a(\lambda)[-2\mathbf{b}(\lambda) + \mathbf{f}_{Ns}(\lambda) + \mathbf{A}\mathbf{b}(\lambda)]\,d\lambda = 0. \quad (40)$$

Because the vector $\mathbf{b}$ is a function of the unknown temperature T_i [see equation (39)], this last equation can be thought of as being a set of simultaneous non-linear equations in T_i. That is, equation (40) is of the form

$$\mathbf{v}(T_1, T_2, \ldots, T_M) = 0, \quad (41)$$

where the vector $\mathbf{v}$ is the L.H.S. of equation (40). The wavelength integration in (40) is performed using a normal cubic spline integrator to accurately account for the absorption band structure. A Newton–Raphson iteration scheme is then applied to the system of equations (41). This scheme converges rapidly to the limit of machine accuracy when an approximate solution [17] is used to start the iterations.

The generality of the present formulation allows the problem space to be almost infinite. An illustrative non-grey medium was therefore chosen to ask two rather general questions and demonstrate the codes capability. The example spectral structure is shown in Fig. 5 and can be viewed as originating from a gaseous absorption coefficient $K_a(\lambda)$. This structure actually comes from the averaged (spectrally smoothed) fundamental vibration–rotation band of carbon monoxide. For simplicity the scattering particles are non-absorbing with a constant scattering coefficient of $K_s = 1\,\text{cm}^{-1}$ and the medium thickness is $X_0 = 1.0\,\text{cm}$. A small temperature difference between the surfaces is chosen for this example ($T_B = 600\text{K}$ and $T_T = 650\text{K}$) to satisfy the assumption of temperature independent properties.

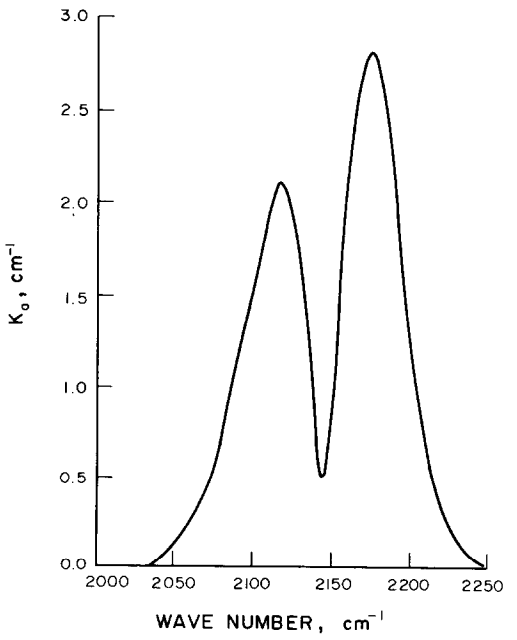

FIG. 5. The CO fundamental absorption band used for the non-grey problems.

The first question asked concerns the accuracy of using grey type models for non-grey problems. To suppress other effects, the scattering is held constant at $g = 0.8$ and the surfaces are black. The non-grey solution of this problem is shown as curve 1 in Fig. 6. The second curve (2) in Fig. 6 is for the same medium but a band-averaged absorption coefficient $\bar{K}_a$ is used instead of the actual absorption coefficient. $\bar{K}_a$ is calculated from

$$\bar{K}_a = \frac{\int_{\Delta\lambda} K_a(\lambda)\bar{B}(\lambda, T_0)\,d\lambda}{\int_{\Delta\lambda} \bar{B}(\lambda, T_0)\,d\lambda}. \quad (42)$$

Here $\Delta\lambda$ is the wavelength range of the absorption band (wavenumbers from 2030 to 2250 cm^{-1}) and $K_a(\lambda)$ is the same as shown in Fig. 5. Once $\bar{K}_a$ is

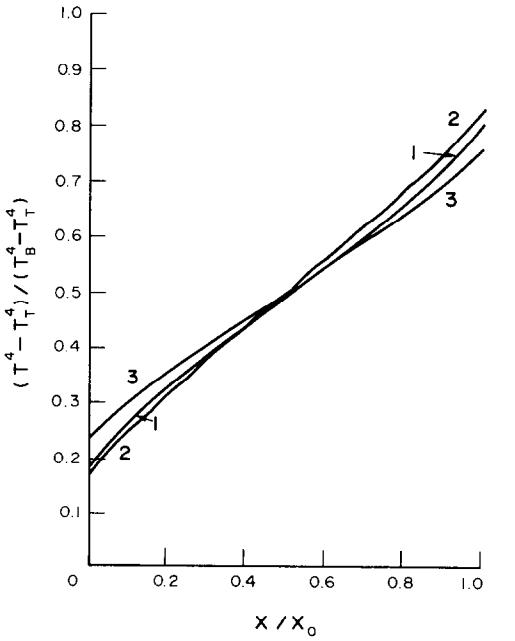

FIG. 6. Temperature as a function of optical depth t for non-grey radiative equilibrium. The medium has the CO absorption coefficient given in Fig. 5 with $K_s = 1\,\text{cm}^{-1}$, $g = 0.8$, $x_0 = 1$ cm, and black surfaces at $T_T = 650$ K and $T_B = 600$ K. The curves correspond to: (1) exact non-grey; (2) a band averaged absorption coefficient, and (3) a grey approximation using the Planck mean absorption coefficient.

calculated, the non-grey medium solution procedure is used to calculate the temperature profile of curve 2 in Fig. 6. This solution simulates the "band model" or "picket fence model" type of solutions for non-grey media (see Ch. 11 in [1]). Curve 3 in Fig. 6 is obtained from a grey approximation for this medium using the Planck mean absorption coefficient K_p defined by

$$K_p = \frac{\pi \int_0^{\infty} K_a(\lambda)\bar{B}(\lambda, T_0)\,d\lambda}{\sigma T_0^4}. \quad (43)$$

where T_0 is given by

$$T_0^4 = \frac{T_B^4 + T_T^4}{2}. \quad (44)$$

Figure 6 shows the inaccuracy of both the band-model approximation and the grey medium assumption for modelling a non-grey absorbing, scattering medium. The grey medium approximation using K_p (curve 3) overestimates the radiation slip and the centerline temperature as compared with the exact solution (curve 1). On the other hand, the solution using $\bar{K}_a$ (curve 2) underestimates the temperature difference between the surfaces and the medium next to them, while predicting a higher centerline temperature than that of the exact solution. The errors involved are of the same order of magnitude as would be introduced by changing the optical depth by about 50% and, therefore, are of importance for many applications.

The second question deals with what are the main effects of media and surface scattering in non-grey radiative equilibrium. Curve 1 in Fig. 7 is the non-grey solution for isotropic scattering ($g = 0.0$) and black surfaces. Curve 2 is the solution for the same conditions except now for anisotropic forward scattering ($g = 0.8$), which is a repeat of curve 1, Fig. 6. Comparing curves 1 and 2 of Fig. 7 shows that forward scatters increase the surface radiation slip as was also observed in the grey solutions of Fig. 3. Similar effects are observed when the optical. depths are decreased, as one would expect from the similarity laws of anisotropic scattering [19]. Curve 3 in Fig. 7 repeats the solution of curve 2 but now for a reflecting bottom surface with the radiative properties given in Fig. 8. Note that in the limit of a completely reflecting bottom surface the medium will take on the top surface temperature T_T everywhere ($\phi = 0.0$). Therefore curve 3 is changing correctly. Curve 4 is the same solution with both surfaces reflecting. As in the discussion for the grey solutions we note that curve 4 is moving towards the limiting case for completely reflecting surfaces of ϕ = constant = 0.5. For these example solutions where the optical depths are small, the scattering effects on the temperature profile are seen to be substantial.

The few example problems solved here do not begin to explore the possible parametric space. They are presented only to illustrate the capabilities of the

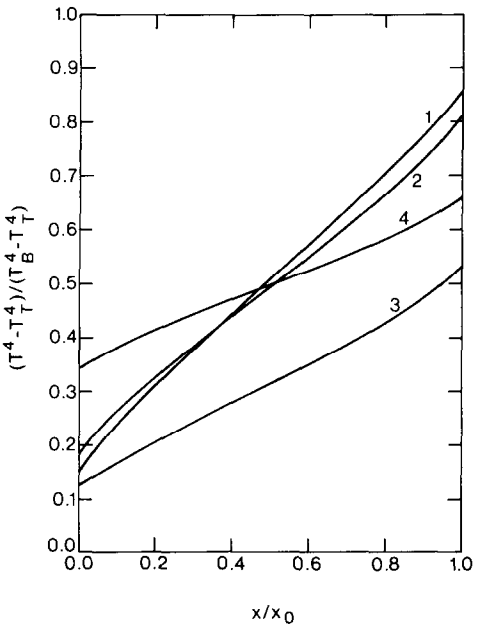

FIG. 7. Same as Fig. 6 except the curves correspond to: (1) $g = 0.0$ and (2) $g = 0.8$, both with black surfaces; (3) reflecting bottom and (4) reflecting top and bottom, both with $g = 0.8$ and surface properties given in Fig. 8.

formulation and computer code. The solution for non-grey radiative equilibrium with scattering presented here is the first solution procedure that is both accurate and general. It has been constructed to accept all possible plane-parallel problems, and therefore is not meant to be compared with simpler approaches that are only valid in special cases. However, the present method is computationally fast (in the range of one cpu minute on an IBM 370) and therefore quite useful for parametric studies.

Combined radiation, conduction and convection

In the preceding section situations in which radiation is the dominant mode of energy transfer have been considered. If conductive heat transfer is also present, the energy equation for 1-dim. media becomes

$$\frac{dq_{RT}}{dx} = k\frac{d^2T}{dx^2}. \quad (45)$$

Here k is the coefficient of thermal conduction for the medium. Expressions for the divergence of the radiative flux appearing above have already been derived [see equations (23), (26) and (28)]. A procedure for numerical solution of (45) is now suggested.

The unknown temperature profile has to be calculated at a finite set of equispaced space locations. Therefore, a discrete representation of the L.H.S. of (45) for the general non-grey case is given by the L.H.S. of equations (40) or (41). The derivative on the R.H.S. of equation (45) can be approximated by a finite difference scheme of the following form:

$$\left.\frac{d^2T}{dx^2}\right|_{x_i} = \frac{T_{i-1} - 2T_i + T_{i+1}}{(\Delta x)^2} + O(\Delta x)^2. \quad (46)$$

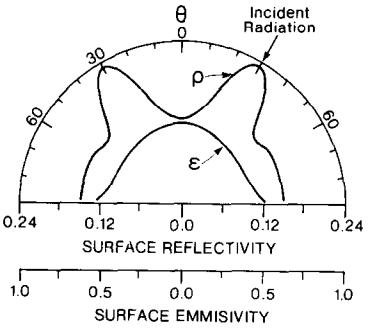

FIG. 8. The bidirectional reflectivity ρ for the incidence angle shown and the corresponding emissivity ε, for the opaque surfaces used in Fig. 7, curves 3 and 4.

In the above expression, Δx is the spacing $(x_i - x_{i-1})$ between the equispaced grid points used. With conduction, the energy equation becomes a set of simultaneous non-linear equations, such that the ith equation is written as

$$\int_0^{\infty} d\lambda K_{a_i}(\lambda) \times \left[-2\bar{B}(\lambda, T_i) + f_{Ns_i}(\lambda) + \sum_{k=1}^{M} A_{ik}(\lambda)\bar{B}(\lambda, T_k) \right] - k\left[\frac{T_{i-1} - 2T_i + T_{i+1}}{(\Delta x)^2} \right] + O[(\Delta x)^2] = 0. \quad (47)$$

The terms appearing above in the integrand have been defined in the section on radiative equilibrium. Because conduction is now present, the boundary conditions require that

$$T_1 = T(x_1) = T_T, \qquad T_M = T(x_M) = T_B. \quad (48)$$

Equation (47) is applicable only to $T_2, T_3, \ldots, T_{M-1}$, and one obtains a system of $(M-2)$ equations in the same number of unknowns. This system of equations can be solved by the same iterative scheme as used in solving equations (40) for radiative equilibrium. Since the equation now involves an approximation for the 2nd-order derivative of T which is accurate only for closely spaced grid points, the temperature would have to be calculated at a larger number of locations (large M).

Even a more complicated problem occurs in the presence of convective heat transfer. In that case the energy equation becomes a partial, differential-integral equation (see, e.g., equation (10-1) of [1]). The radiative transfer formulation discussed here may be used to substitute for the divergence of radiative heat flux in the energy equation. However, this results in a problem difficult to solve unless simplifying assumptions are made. Further analysis of this problem, and actual solution of the combined radiation and conduction problem using the method outlined here are left to future research.

CONCLUDING REMARKS

This paper has presented a new method for solving radiative heat transfer problems in plane-parallel media with anisotropic scattering. The particular problem of radiative equilibrium was solved for a non-grey, scattering medium. The numerical computer programs developed in the course of this work are rather fast and can be used for many other studies, since the formulation is completely general. These codes are available from the authors.

The real limitation of the present formulation is that it applies only in plane-parallel geometry. There are indications that a similar 3-dim. approach could be developed [20, 21]. Although this would not be a simple project, it is probably the only method that will lead to general solutions of radiative transfer with scattering in multi-dimensional media with arbitrary surfaces.

REFERENCES

1. E. M. Sparrow and R. D. Cess, *Radiation Heat Transfer* (Augmented Edition), pp. 203–271. McGraw-Hill, New York (1978).
2. R. Viskanta and R. J. Grosh, Heat transfer in thermal radiation absorbing and scattering medium, *Int. Heat Transfer Conf., Boulder, CO, 1961*, p. 820.
3. W. Lick, Transient energy transfer by radiation and conduction, *Int. J. Heat Mass Transfer* **8**, 119–127 (1965).
4. M. A. Heaslet and R. F. Warming, Radiative transport and wall temperature slip in an absorbing planar medium, *Int. J. Heat Mass Transfer* **8**, 979–994 (1965).
5. R. D. Cess and A. E. Sotak, Radiation heat transfer in an absorbing medium bounded by a specular reflector, *Zamp* **15**, 642–647 (1964).
6. A. L. Crosbie and R. Viskanta, Non-grey radiative transfer in a planar medium exposed to a collimated flux, *J. quant. Spectrosc. radiat. Transfer* **10**, 465–485 (1970).
7. S. Chandraskekhar, *Radiative Transfer*. Dover, New York (1960).
8. A. Sharma, An Accurate and Computationally Fast Formulation for Radiative Fields and Heat Transfer in General, Plane-Parallel, Non-Grey Media with Anisotropic Scattering. Ph.D. Thesis, University of Illinois at Chicago Circle, Chicago (1980).
9. A. C. Cogley and A. Sharma, A General and Computationally Fast Formulation for Radiative Transfer with Scattering, Proc. AIAA 14th Thermophysics Conf., Orlando, AIAA Paper No. 79-1035, 1979.
10. A. C. Cogley, Adding and invariant imbedding equations in matrix notation for all the scattering functions, *J. quant. Spectrosc. radiat. Transfer* **19**, 113–126 (1978).
11. A. C. Cogley, Derivation and application of the reciprocity relations for radiative transfer with internal illumination, *J. quant. Spectrosc. radiat. Transfer* **15**, 749–760 (1975).
12. H. M. Domanus and A. C. Cogley, A fundamental-source-function formulation of radiative transfer and the resulting fundamental reciprocity relations, *J. quant. Spectrosc. radiat. Transfer* **14**, 705 (1974).
13. A. C. Cogley and R. W. Bergstrom, Numerical results for the thermal scattering functions, *J. quant. Spectrosc. radiat. Transfer* **21**, 263 (1979).
14. G. E. Hunt, A review of computational techniques for analyzing the transfer of radiation through a model cloudy atmosphere, *J. quant. Spectrosc. radiat. Transfer* **11**, 655 (1971).

15. W. J. Wiscombe, Extension of the doubling method to inhomogeneous sources, *J. quant. Spectrosc. radiat. Transfer* **16,** 477 (1976).
16. A. Sharma, A. C. Cogley and S. Tonon, A parametric error analysis of the adding/doubling method for radiative scattering in inhomogeneous media, *J. quant. Spectrosc. radiat. Transfer,* **26,** 39–48 (1981).
17. A Sharma and A. C. Cogley, Numerical techniques for radiative heat transfer in general, scattering media, to be publihed in *Numerical Heat Transfer.*
18. J. E. Hansen, Exact and approximate solutions for multiple scattering by cloudy and hazy planetary atmospheres, *J. atmos. Sci.* **26,** 478 (1969).
19. V. V. Sobolev, *Light Scattering in Planetary Atmospheres.* p. 158, Pergamon Press, New York (1975).
20. R. W. Preisendorfer, *Radiative Transfer on Discrete Spaces.* Pergamon Press, London (1965).
21. F. R. Mosher, Visible Flux Variations Across Finite Clouds. Ph.D. Thesis, University of Wisconsin, Madison (1979).

TRANSFERT DE CHALEUR PAR RAYONNEMENT DANS UN ENVIRONNEMENT QUELCONQUE A PLANS PARALLELES

Résumé—On présente une nouvelle approche du transfert radiatif avec diffusion et on obtient la première solution générale pour un milieu non gris immobile entre deux plans parallèles. On discute aussi l'utilisation de la méthode en incluant la conduction et la convection. Des champs radiatifs sont calculés à l'aide de fonctions de diffusion (fonctions de Green) qui représentent la réponse du milieu et des surfaces diffusantes (réflectrices) quelconques à un rayonnement de type unitaire. Ces fonctions de diffusion sont déterminées en utilisant une méthode numérique rapide. L'équation de conservation d'énergie contenant ces fonctions de diffusion est ensuite résolue numériquement pour n'importe quel problème de thermique.

WÄRMEÜBERGANG DURCH STRAHLUNG IN EINER VOLLKOMMEN ALLGEMEINEN PLANPARALLELEN UMGEBUNG

Zusammenfassung—Es wird ein neuer Ansatz zur Beschreibung des Strahlungswärmeaustausches mit Streuung vorgestellt und auf die Entwicklung der ersten allgemeinen Lösung für das Strahlungsgleichgewicht in einem nicht-grauen planparallelen Medium angewandt. Die Anwendung der Methode bei Berücksichtigung von Leitung und Konvektion wird ebenfalls diskutiert. Diffuse Strahlungsfelder werden in Form von definierten Streufunktionen (Greenschen Funktionen) berechnet, welche das Verhalten des Mediums und aller streuenden (reflektierenden) Oberflächen bei Einheitsbeleuchtung beschreiben. Die Streufunktionen werden mit Hilfe eines schnellen numerischen Verfahrens gefunden. Die Energie–Erhaltungs-Gleichung, die diese Streufunktionen enthält, wird dann numerisch für jedes spezielle Wärmeübergangsproblem gelöst.

ЛУЧИСТЫЙ ТЕПЛОПЕРЕНОС В ОБЩЕМ СЛУЧАЕ ПЛОСКОПАРАЛЛЕЛЬНЫХ ОГРАЖДАЮЩИХ ПОВЕРХНОСТЕЙ

Аннотация — Предложен новый метод исследования лучистого теплопереноса в присутствии рассеяния и с его помощью впервые получено общее решение равновесного излучения в несерой плоскопараллельной среде. Рассмотрена также возможность использования метода при учете передачи тепла теплопроводностью и конвекцией. Диффузные лучистые поля рассчитываются с помощью функций рассеяния (функций Грина), характеризующих влияние однородной освещенности на среду и рассеивающие (отражающие) поверхности. Функции рассеяния определяются численно методом быстрого суммирования. Затем уравнение сохранения энергии, содержащее эти функции, решается численно для любой задачи теплообмена.